ISSN 1027-4510, Journal of Surface Investigation: X-ray, Synchrotron and Neutron Techniques, 2019, Vol. 13, No. 5, pp. 985–989. © Pleiades Publishing, Ltd., 2019.

Preparation and Adsorptive Performance of Transition Metal Oxide Nanoparticles in Removal of Fe(III) Ions

Zh. Farhadravesh[a], N. Samadani Langeroodi[a, *, **], and A. D. Khalaji[a]

[a] *Department of Chemistry, Faculty of Sciences, Golestan University, Gorgan, Iran*

**e-mail: n.samadani@gu.ac.ir*

***e-mail: nsamadani@yahoo.com*

Received December 12, 2018; revised January 3, 2019; accepted March 23, 2019

Abstract—In this study, we focus on preparation and adsorptive performance of transition metal oxide nanoparticles in removal of Fe(III) ions. The prepared nanoparticles including iron oxide (Fe_2O_3), cobalt oxide (Co_3O_4) and manganese oxide (Mn_2O_3/Mn_3O_4) nanocomposite provide a good affinity for Fe(III) ions adsorption from aqueous systems. Among them, Fe(III) ions were adsorbed by manganese oxide (Mn_2O_3/Mn_3O_4) nanocomposite with a higher removal ratio compared to the other nanoparticles.

Keywords: transition metal oxides, nanoparticles, adsorption, FT-IR spectroscopy, X-ray diffraction, FE-SEM

DOI: 10.1134/S1027451019050276

1. INTRODUCTION

Heavy metals, such as Pb(II) and Cd(II), are one of the main classes of released pollutants [1, 2]. Since heavy metals are non-biodegradable and may accumulate in living tissues, their removal from wastewaters is legally imposed, nowadays [2, 3]. One of the major heavy metals that should be removed is Iron. Iron plays a significant role in oxygen transport and storage, in living systems. Iron ions existing in environmental water originate from steel tempering, coal coking and mining industries [4]. Iron toxicity can cause anorexia, oligura and diphasic shock. Iron overdose, known as hemochromatosis, is caused by a gene that enhances iron absorption in body [5]. Iron accumulates over time in liver, bone marrow, pancreas, skin and testicles. Accumulation of iron in these organs makes them functions poorly [6, 7]. One of the best methods for removal of heavy metal pollutants from aqueous solution is adsorption. Adsorption process is considered as one of the most efficient, economical and preferred techniques for purification of water due to possibility of synthesizing cheap adsorbents, flexibility in design and facile handling. Among the available adsorbents, metal oxide nanoparticles, which are often characterized by significant amounts of surfaces and high capacities, are classified as promising adsorbents for heavy metal removal because of their unique properties and potential applications [8, 9]. Various papers related to removal of heavy metals have been reported that have used metal oxide nanoparticles, e.g. magnetic nano-or micro particles, manganese oxide, aluminum oxides and magnesium oxides [8–11].

The aim of this work is synthesis of transition metal oxide nanoparticles of α-Fe_2O_3, Co_3O_4 and Mn_2O_3/Mn_3O_4 nanocomposite and applying them to adsorption of Fe(III) ions. The nanoparticles were synthesized by sol-gel method and characterized by IR, BET, SEM and XRD techniques.

2. EXPERIMENTAL

2.1. Materials and Methods

Chemical reagents, such as $Mn(NO_3)_2 \cdot 4H_2O$, $Co(NO_3)_2 \cdot 6H_2O$, $Fe(NO_3)_3 \cdot 9H_2O$, and solvents, were purchased from Merck in high purities and used as received without any further purifications. Fourier transform infrared (FTIR) analysis of the metal oxides was performed with a FTIR spectrometer (Perkin-Elmer Model System 2000 using KBr pellet method). In order to observe surface morphology of the biosorbents directly, FE-SEM (Field emission scanning electron microscopy) (SIGMA VP-500, Germany) was employed, in this study. Elemental information and structure of the synthesized materials were determined by a X-ray diffractometer (XRD) (X' Pert Pro, Panalytical, Netherlands), at an ambient temperature. Specific surface area of the particles was measured by a Brunauer, Emmett and Teller (BET) surface area analyzer (Nova Station A, Quantachrome, America) by nitrogen adsorption. Unabsorbed Fe(III) ions,

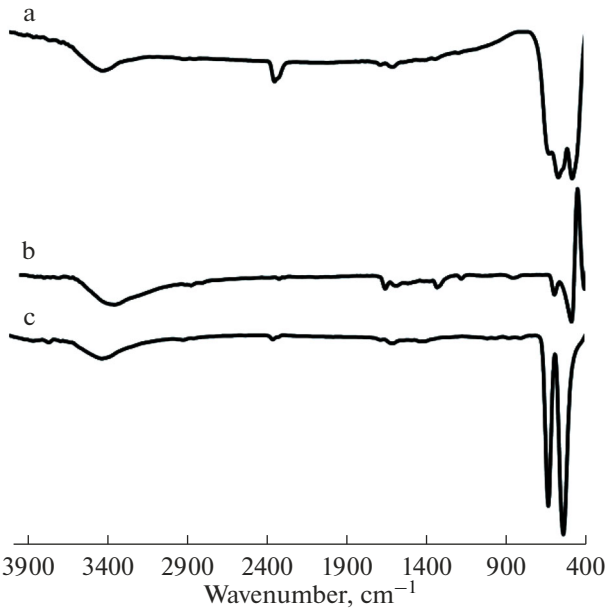

Fig. 1. FT-IR spectra of (a) Mn_2O_3/Mn_3O_4 nanocomposite, (b) α-Fe_2O_3, and (c) Co_3O_4.

remaining in the supernatant liquid, were quantified with Atomic Absorption Spectrometer (model Shimadzu, AA-7000).

2.2. Preparation of the Nanoparticles

In the laboratory, the transition metal oxide nanoparticles were prepared by sol-gel method. First, 5 g of the desired metal salt was dissolved in 75 mL of deionized water. Then, 1 M NaOH solution was added drop wise into the mixture with mechanical stirring, at room temperature. When pH reached 13, the stirrer was turned off and the obtained solution was kept at room temperature for 24 hours. After this time, the content was filtered and washed several times with deionized water to remove any NaOH and the wet powders were dried, at 70°C for 18 hours. The obtained dry powder was heated in a quartz tube furnace, at 250°C for 3 hours. Finally, the powder was calcinated for 3 hours, at 600°C.

2.3. Batch Tests

Batch adsorption studies were performed by mixing 0.4 g of the nanoparticles with 200 mL of 10 mg L^{-1} $Fe(NO_3)_3 \cdot 9H_2O$ solution. The suspensions were equilibrated by shaking for a desired period of time. The clear supernatants, which were obtained after filtration, were analyzed for Fe(III) concentrations using an atomic absorption spectrometer. Removal ratio of metal ions was calculated using the following equation:

$$\eta = \frac{C_0 - C_e}{C_0} \times 100, \quad (1)$$

where C_0 (mg dm^{-3}) and C_e (mg dm^{-3}) are the initial and equilibrium concentrations of the adsorbate, respectively and η is the removal ratio (in percent) of Fe(III).

3. RESULTS AND DISCUSSION

3.1. FT-IR Spectroscopy

The FT-IR spectra (Fig. 1) of iron oxide (α-Fe_2O_3), cobalt oxide (Co_3O_4) and manganese oxide (Mn_2O_3/Mn_3O_4) nanocomposite are shown in the IR spectra of Mn_2O_3/Mn_3O_4, the stretching vibration band, located at 588 cm^{-1} corresponds to vibration of Mn–O in an octahedral environment while the stretching vibration band located at 484 cm^{-1} can be attributed to vibration of manganese species (Mn^{3+}–O) in the octahedral site of Mn_3O_4. The stretching vibration band at 484 cm^{-1} confirmed presence of Mn_2O_3 [12, 13]. The characteristic adsorption bands positioned at 605 and 497 cm^{-1} are assigned to Fe–O stretching and bending vibration modes of α-Fe_2O_3, respectively [14, 15]. It can be seen that α-Fe_2O_3 shows two peaks, which are related to its structure and size. Finally, the IR spectrum of Co_3O_4 nanoparticles displays two distinctive bands that originate from stretching vibrations of Co-oxygen bond. The adsorption bond that is appeared at 632 cm^{-1} was assigned to stretching vibration mode of Co^{II}–O in a tetrahedral hole and the peak observed at 538 cm^{-1} was assigned to stretching vibration mode of Co^{III}–O in an octahedral hole [16–18].

3.2. X-ray Diffraction

The crystalline structures of these nanoparticles were characterized by X-ray powder diffraction. The X-ray powder diffraction patterns of manganese oxide (Mn_2O_3/Mn_3O_4) nanocomposite, iron oxide (α-Fe_2O_3) and Co_3O_4 are shown in Fig 2. The average crystallite sizes of the samples were calculated from their X-ray powder diffraction line broadenings using Scherrer's formula:

$$d = 0.9\lambda/\beta\cos\theta, \quad (2)$$

where d is the crystallite size (nm), θ is the angle of incidence, λ is wavelength of X-ray diffraction (λ = 1.5406 nm) and β is full width at half maximum [19]. The average crystallite sizes of the nanoparticles are about 27, 47 and 48 nm, respectively.

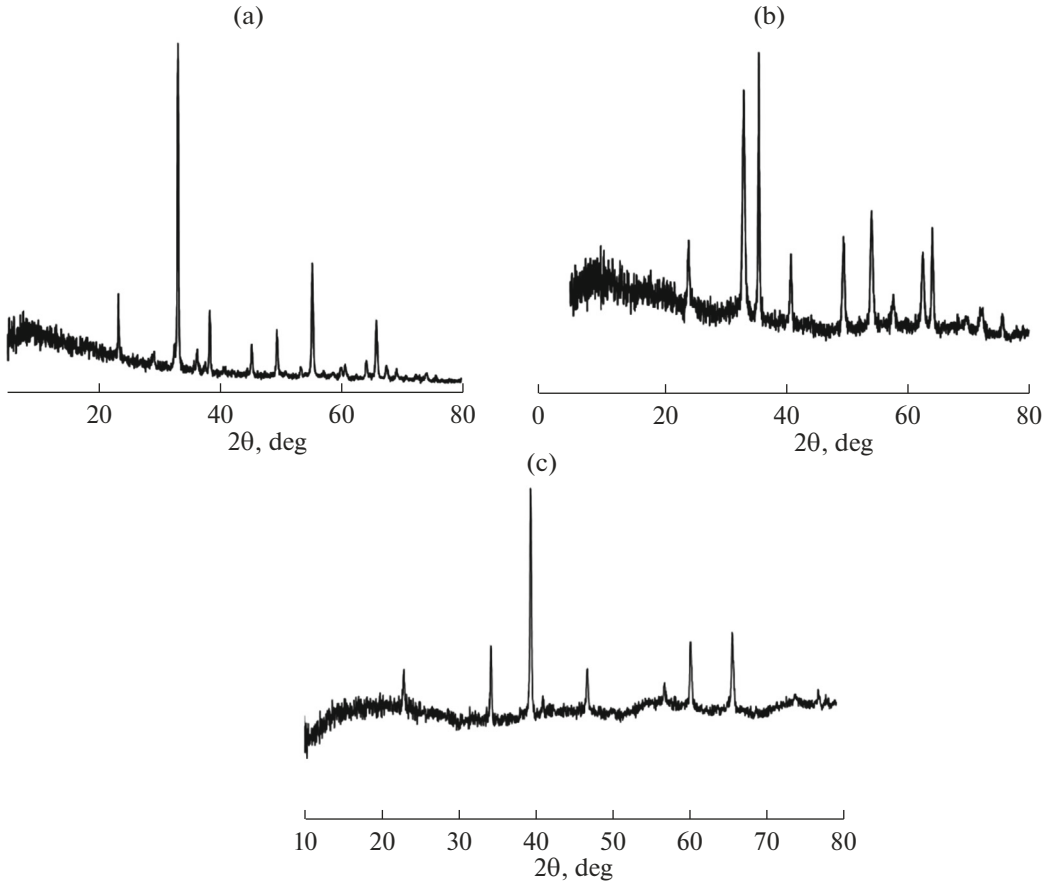

Fig. 2. X-ray powder diffraction patterns of (a) Mn_2O_3/Mn_3O_4; (b) α-Fe_2O_3, and (c) Co_3O_4.

From Fig. 2a, the peak positions at $2\theta = 23.33°$, 33.14°, 38.41°, 45.34°, 49.53°, 55.35°, and 65.93° confirmed preparation of Mn_2O_3/Mn_3O_4 nanocomposite (JCPDS: 10-0069, 24-0734) with a cubic structure while the peak positions at $2\theta = 24.33°$, 33.34°, 35.81°, 41.05°, 49.65°, 54.24°, 57.78°, 62.61°, 69.68°, 72.16° and 75.60° (Fig. 2b) approved preparation of α-Fe_2O_3 nanoparticle (JCPDS: 33-0664) with a cubic structure [14, 20]. Finally, the peak positions at $2\theta = 19.08°$, 31.35°, 36.93°, 38.66°, 44.89°, 59.41° and 65.31° verified synthesis of Co_3O_4 nanoparticles (JCPDS: 43-1003) (Fig. 2c) with a cubic structure. X-ray powder diffraction results showed that the prepared nanoparticles are well crystalline materials.

3.3. SEM Images

Figure 3 shows SEM images of the synthesized nanoparticles. The SEM image of Mn_2O_3/Mn_3O_4 nanocomposite (Fig. 3a) confirmed spherical or approximately spherical morphology of this nanoparticle with a multilayer macro porous surface, which can be beneficial for metal ion diffusion and adsorption.

As observed in Fig. 3b, the obtained α-Fe_2O_3 nanoparticles exhibit almond like structures (rod shape). It seems that agglomerated particles were obtained. The SEM image revealed the nature of the surface of this adsorbent as a multilayer surface with irregular laminated structure and low number of micro pores.

SEM image of Co_3O_4 nanoparticles (Fig. 3c) showed spherical and partly almond like structures. The SEM image revealed nature of the surface of this adsorbent as a multilayer porous surface with a limited number of micro and meso pores.

3.4. Adsorptive Properties of the Prepared Nanoparticles

Results of Fe(III) adsorption by the prepared nanoparticles are presented in Table 1. The results indicated that Mn_2O_3/Mn_3O_4 nanocomposite provides the highest removal ratio of Fe(III) ion, as compared with the other nanoparticles prepared in this study. Such an observation could be due to the multilayer porous surface of manganese oxide nanocom-

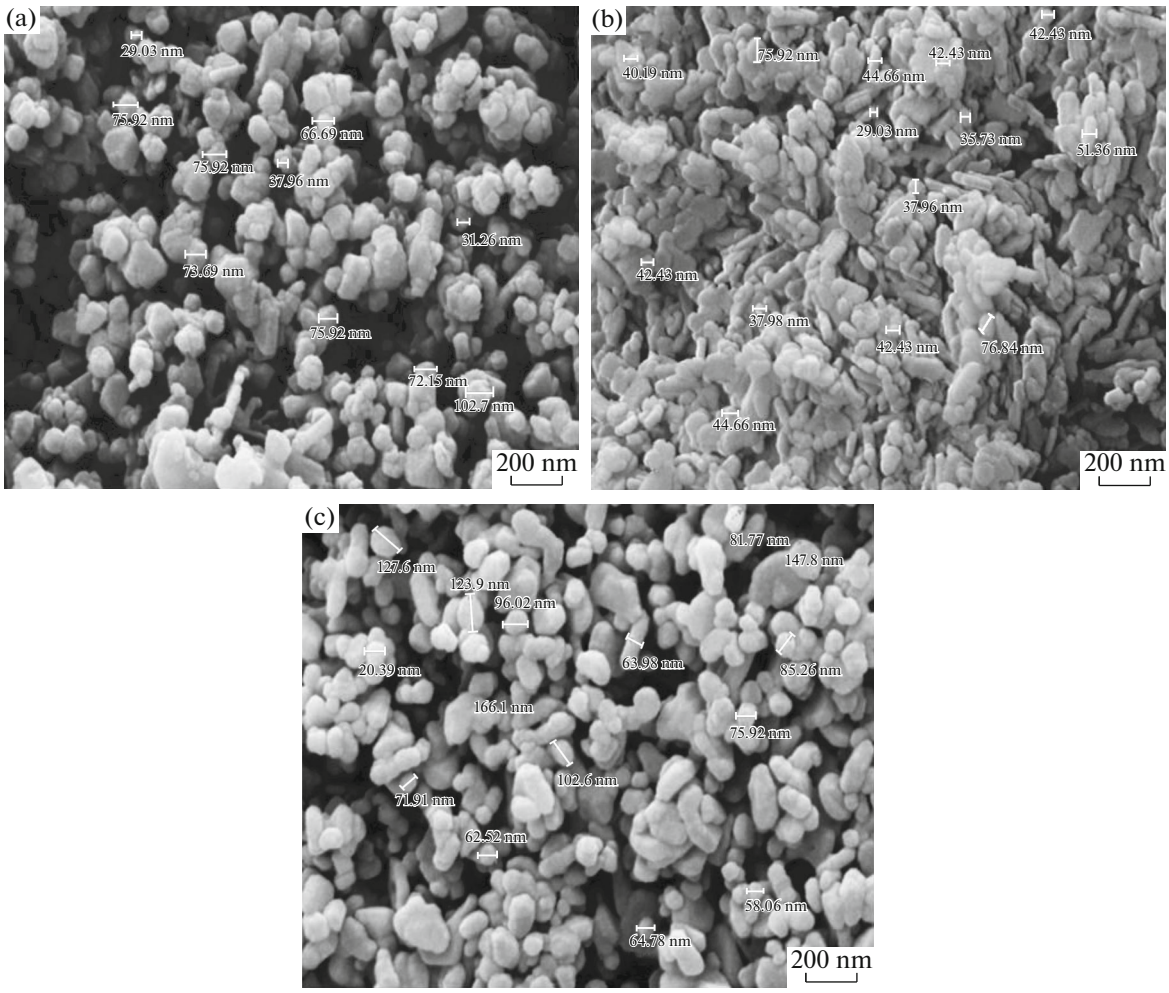

Fig. 3. SEM images of (a) Mn_2O_3/Mn_3O_4, (b) α-Fe_2O_3, and (c) Co_3O_4.

posite, which can be beneficial to diffusion and adsorption of metal ions despite its lower surface area.

CONCLUSIONS

In this study, Mn_2O_3/Mn_3O_4 nanocomposite, and α-Fe_2O_3 and Co_3O_4 nanoparticles were synthesized by sol-gel approach and characterized by IR, SEM, and XRD methods. Also, BET surface areas of them were determined. Compared with Co_3O_4 and α-Fe_2O_3 nanoparticles, Mn_2O_3/Mn_3O_4 nanocomposite was more effective in removing Fe(III) ions from aqueous solution in the adsorption process because of its suitable crystallinity and multilayer porous surface.

Table 1. Adsorption properties of the prepared nanoparticles

Adsorbent	Removal ratio, %	Surface area, $m^2\ g^{-1}$
Mn_2O_3/Mn_3O_4	85.6	15.53
α-Fe_2O_3	61.2	39.99
Co_3O_4	73.8	21.39

FUNDING

The authors would like to appreciate Golestan University for providing financial support of the work described in this paper.

REFERENCES

1. N. N. Nassar, J. Hazard. Mater. **184**, 538 (2010).
2. Y. Feng, J. L. Gong, G. M. Zeng, Q. Y. Niu, et al., Chem. Eng. J. **162**, 487 (2010).
3. C. Han, H. Pu, H. Li, L. Deng, et al., J. Hazard. Mater. **254–255**, 301 (2013).
4. Z. Aksu, A. Calik, A. Y. Dursum, and Z. Demircan, Process. Biochem. **34**, 483 (1999).
5. K. G. Bhattacharyya and S. S. Gupta, Adsorption **12**, 185 (2006).
6. W. S. Wan Ngah, S. Ab Ghani, and A. Kamari, Biores. Technol. **96**, 443 (2005).

7. S. Hashemian, S. H. Hosseini, H. Salehifar, and Kh. Salari, Am. J. Anal. Chem. **4**, 123 (2013).
8. M. A. El-Sayed, Acc. Chem. Res. **34**, 257 (2001).
9. E. A. Deliyanni, E. N. Peleka, and K. A. Matis, J. Hazard. Mater. **172**, 550 (2009).
10. A. Agrawal and K. K. Sahu, J. Hazard. Mater. **137**, 915 (2006).
11. M. Hua, Sh. Zhang, B. Pan, W. Zhang, and L. Lv, J. Hazard. Mater. **211–212**, 317 (2012).
12. H. Dhaouadi, O. Ghodbane, F. Hosni, and F. Touati, ISRN Spectrosc. **2012,** Art. Id 706398 (2012).
13. M. Salavati-Niasari, M. Esmaeili-Zare, and M. Gholami-Daghian, Advanc. Powder Technol. **25**, 879 (2014).
14. Y. F. Shen, J. Tang, Z. H. Nie, Y. D. Wang, et al., Sep. Purif. Technol. **68**, 312 (2009).
15. S. K. Sahoo, K. Agarwal, A. K. Singh, B. G. Polke, and K. C. Raha, Int. J. Eng. Sci. Technol. **2**, 118 (2010).
16. S. H. Wu, and D. H. Chen, J. Colloid. Interface. Sci. **259**, 282 (2003).
17. L. Estepa, and M. Daudon, Biospectroscopy **3**, 347 (1997).
18. R. Manigandan, K. Giribabu, R. Suresh, L. Vigayalakshmi, et al., Chem. Sci. Trans. **2** (S1), S47 (2013).
19. M. Abareshi, E. K. Goharshadi, S. M. Zebarjad, H. K. Fadafan, and A. Yussefi, J. Magn. Mater. **322,** 3895 (2010).
20. H. Cui, Y. Liu, and W. Ren, Adv. Powder. Technol., **24,** 93 (2013).